scientific reports

OPEN

Numerical simulation of hydrochemical evolution of deep pore thermal reservoirs in shallow groundwater recharge of Yancheng uplift

Zhao Mingkun[1,2,3,4], Du Xiaochong[2,5], Qiang Shanfeng[2,5], Jiang Min[6 ✉], Bi Guangxu[2,5], Tang Xin[7] & Duan Zhongfeng[8 ✉]

This article relies on PHREEQC software, the hydrochemical model of the main development thermal reservoir of shallow groundwater recharge is constructed by using the dissolution kinetic rate formula. The 120-day recharge period is used to simulate the change of the hydrochemical composition of the thermal reservoir within one year. Simulation results indicate that allochthonous recharge sources have modified the hydrochemical characteristics of the geothermal reservoir within a specific range. During the recharge process, the hydrochemical field is mainly controlled by water runoff and dispersion. Taking the recharge well as the center, the hydrochemical type on the radial direction gradually changes from Na-HCO$_3$•SO$_4$•Cl to Na-HCO$_3$•Cl•SO$_4$, Na-Cl•HCO$_3$•SO$_4$, Na-Cl•SO$_4$•HCO$_3$, Na-Cl•SO$_4$, Na-Cl•SO$_4$•HCO$_3$, Na-Cl•SO$_4$ gradually changes into Na-Cl type, showing a trend of gradual transition from recharge to geothermal water in hot reservoirs. After the recharge stopped, the hydrochemical type near the recharge well changed from runoff and dispersion control to water-rock reaction and dispersion control. Continuous reinjection for 120 days induced a 0.35% reduction in reservoir porosity and permeability attenuation. Structural deterioration intensified after reinjection cessation, with porosity decline reaching 3.35% by 180 days, indicating irreversible pore structure degradation in the thermal reservoir.

With the development of China's economy and the improvement of people's material living standards, the demand for energy is also constantly increasing[1]. As a traditional energy source, fossil energy supports the early social and economic development, but its production and consumption activities have always been considered as the main source of carbon emissions. With the continuous increase of global energy consumption, the corresponding environmental problems are becoming more and more prominent[2], such as greenhouse effect, extreme climate, environmental pollution, etc.

The 2014 Sino US Joint Statement on Climate Change proposed that China aims to achieve a 20% share of non fossil energy in primary energy by 2030; In September 2020, China also proposed the "dual carbon goals" of peaking carbon emissions before 2030 and achieving carbon neutrality before 2060[3], all of these require that the proportion of new energy in China 's existing energy structure should be greatly increased. As a non-carbon-based energy source with no pollution, renewable, wide distribution and abundant resources[4], geothermal

[1]School of Resources and Civil Engineering, Suzhou University, Suzhou 234000, China. [2]Key Laboratory of Water and Soil Resources Conservation and Restoration in the Middle and Lower Reaches of Yellow River Basin, Ministry of Natural Resources, Zhengzhou 450016, China. [3]Anhui Wanbei Coal Power Group Co., Lid., Suzhou 234000, China. [4]School of Resources and geosciences, China University of Mining and Technology, Xuzhou 221116, Jiangsu, China. [5]Henan Academy of Geology, Zhengzhou 450016, China. [6]Chongqing Surveying and Mapping Institute Co., Ltd., Chongqing 40010, China. [7]Civil Engineeringy, Chongqing Three Gorges Universit, Wanzhou 404100, Chongqing, China. [8]School of Geosciences, China University of Petroleum(East China), Qingdao 266580, China. ✉email: 208944874@qq.com; 1152443994@qq.com

energy shows great potential for development and utilization in the critical period of promoting high-quality economic development and achieving the phased goal of ' double carbon ' in China, which can provide an important guarantee for achieving this goal[5].

According to the survey and evaluation results of China Geological Survey, the annual recoverable resources of shallow geothermal energy in China are equivalent to 700 million tons of standard coal, while the annual recoverable resources of hydrothermal geothermal energy are equivalent to 1.865 billion tons of standard coal under the premise of recharge. The basic resources of dry hot rock between 3 km and 5.5 km are equivalent to 106 trillion tons of standard coal, and the basic resources of dry hot rock between 5.5 km and 10 km are equivalent to 750 trillion tons of standard coal[5,6].The reserves of various types of geothermal energy resources are huge.

In particular, hydrothermal geothermal energy, because of its wide distribution and low development technical difficulty, has been developed on a large scale in plains and basins such as Shandong[7], Henan[8], Shaanxi[9], Hebei[10], and Xiong'an New Area[11].

Hydrothermal geothermal resources are dual-type resources of water and heat. In the early stage, the understanding of hydrogeological conditions such as recharge, runoff and discharge is insufficient. The unbalanced recharge of long-term mining has caused the water level of thermal reservoirs to drop seriously. For example, the water level of Xi 'an thermal reservoir has dropped from 16.5m to nearly 200m[12], and the water level of main thermal reservoirs such as Tianjin and Xiong 'an has also dropped by nearly 100m[6],The water level of the lower member of Minghuazhen Formation in the main heat mining reservoir of Yancheng uplift decreased from the original water level of 30 m to 120 m[3].

The sharp decline in the water level of the thermal reservoir not only causes a reduction in production capacity, but also causes increases the cost of resource development, and leads to geological disasters such as land subsidence[13], which has caused the government and society to worry about the deterioration of the geological environment.

In 1969, since the first attempt to recharge the Geyser geothermal field in California[14], this technology has been applied to varying degrees in the United States[15–17], New Zealand[18], Iceland[19,20], Italy[21,22], Japan[23–26], Romania[27], Philippines[28], Ethiopia[29], Denmark[30], Costa Rica[31], Kenya[32], Croatia[33], Mexico[34], El Salvador[35], Russia[36], and France[37] and other countries. Reinjection has gradually become an important technical means for the sustainable development and utilization of hydrothermal geothermal resources, and research on geothermal reinjection has gradually increased.

However, scholars often focus on porosity changes and particle arrangement[38], reservoir blockage[39], reservoir damage[39–41],scaling improvement of reinjection wells[42], chemical stimulation[43], etc., and pay more attention to geothermal energy utilization efficiency and duration. There are few studies on the changes of groundwater chemical field caused by recharge. Only scholars such as Li Shengtao[44] and Xue Meiping[45] have conducted numerical simulation analysis on the hydrochemical evolution of cross layer recharge and mine water recharge in deep karst thermal reservoirs.

The thermal reservoir development of the Minghuazhen Formation in the Yancheng uplift has caused a water level drop of nearly 90 m, and its geothermal water use is single, bathing and domestic water accounts for 99%[3], and it does not have tail water recharge conditions for the time being.In this study, the shallow groundwater recharge thermal reservoir is used as the working condition to study the hydrochemical evolution of the thermal reservoir under the recharge condition, so as to explore the possibility of heterogeneous water recharge to repair the thermal reservoir.

Overview of the Yancheng uplift

The working area is located in the Pingdingshan-Yancheng uplift conductive geothermal field in the Zhoukou sag basin in the Songji tectonic area of the North China plate. The thickness of Minghuazhen Formation is 1100 ~ 1200 m, and the floor elevation is -1150 ~ 1650 m. It is deep in the East and shallow in the West. It is mainly a set of fluvial-lacustrine facies deposits, including interbedded layers of varying thicknesses of brown-red, brown-yellow, gray-white, gray-green mudstone, sandy mudstone, siltstone, sandstone, and pebbled sandstone.The structural position and structural form of the working area are shown in Fig. 1.The northern part of the study area is the Shaling-Shangqiao sag, the southern part is the Xiping sag, and the eastern part is the Shenqiu sag. The overall structural form of the "three depressions surrounded by one uplift" is a favorable area for geothermal development.

Overview of recharge experiment

As shown in Fig. 1, the recharge site is located in the east of Yancheng uplift. The recharged thermal reservoir is the lower member of Minghuazhen Formation in Neogene. The depth of the recharged geothermal well TM1 is 1402.48 m, and the thickness of the thermal reservoir is 118.52 m. The lithology of the thermal reservoir is mainly weakly cemented siltstone, fine-grained sandstone, grain-bearing coarse sandstone and mudstone thin layer, as shown in Fig. 2. The type of thermal reservoir is porous thermal reservoir. According to the actual measurement of this work, the depth of the constant temperature zone in Yancheng uplift is 20 ~ 26 m, and the temperature of the constant temperature zone is 16.4 ~ 16.7 °C.This time, the depth of the constant temperature zone is 22 m, the temperature of the constant temperature zone is 16.6 °C (the annual average temperature of the study area is 14.6 °C), the average ground temperature gradient is 3.6 °C / 100 m, and the average temperature of the thermal reservoir is 60 °C.

The rock composition and physical properties of the thermal reservoir were tested by the Institute of Rock Mechanics, Chinese Academy of Sciences. The main components of the rock were analyzed by X-ray diffraction,
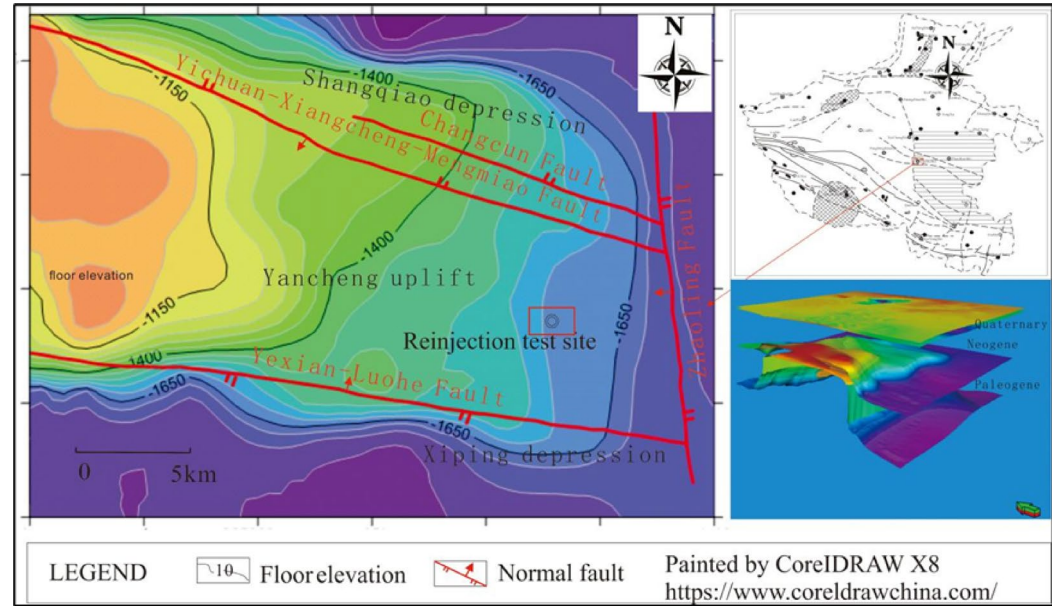
Fig. 1. Structural map and contour map of the base of the Minghuazhen Formation(The map outline in the figure is based on reference)[46].
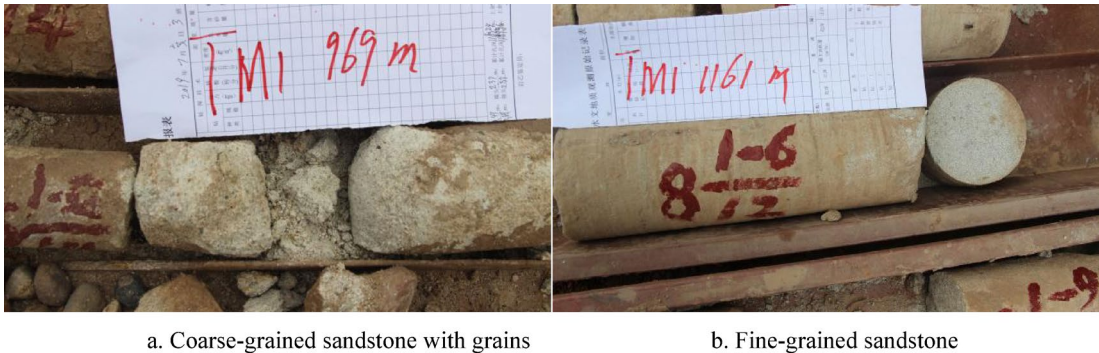

a. Coarse-grained sandstone with grains   b. Fine-grained sandstone

Fig. 2. Core of the Geothermal Reservoir.

Depth(m)	Clay (%)	Quartz (%)	K- Feldspar (%)	Plagioclase (%)	Calcite (%)	Dolomite (%)	Limonite (%)	Dolomites (%)	Muscovite (%)
1157.80–1158.00	7.8	78.3	7.5	4.3	1.1				
1219.38-1219.53	30.1	53.7	4.8	2.9	5.2	3.4			
1266.87-1267.07	31.6	41.1	3.5	5.2	13.7		1.5		
1271.17-1271.32	20.1	44.1	3.3	6.3	21.1		1.1		
1297.00-1297.20	8.8	59.7	9.1	14.1	6.9			1.4	
1332.10-1332.25	33.9	31.0	5.2	5.4	13.6		2.3	3.6	5.0
1334.00-1334.15	24.1	41.1	3.7	12.5	12.7				5.9

Table 1. The composition of reservoir rocks.

mainly clay minerals, quartz, potassium feldspar, plagioclase and calcite. The rock composition is shown in Table 1. The average density of thermal reservoir is 2.42 g / cm³, and the average porosity is 18.53%.

The recharge water source is a shallow water well with a depth of 25 m 15 m east of the geothermal well. The Quaternary diving water is taken from the recharge water source well to recharge the geothermal well. Before recharge, the WH-SLB50 / 5 – 1 large flow filter is used to filter the recharge water, and the filtration accuracy can reach 2 μm. The recharge method is gravity recharge. The recharge temperature is 20 °C, and the recharged

Name	Na⁺ (mg/L)	K⁺ (mg/L)	Mg²⁺ (mg/L)	Ca²⁺ (mg/L)	Cl⁻ (mg/L)	SO₄²⁻ (mg/L)	HCO₃⁻ (mg/L)
Reinjection water	596	4	12	123	87	124	286.58
Geothermal water	875	13	34	236	1416	586	140.65

Table 2. The chemical compositions of the geothermal well water and the reinjection well water.
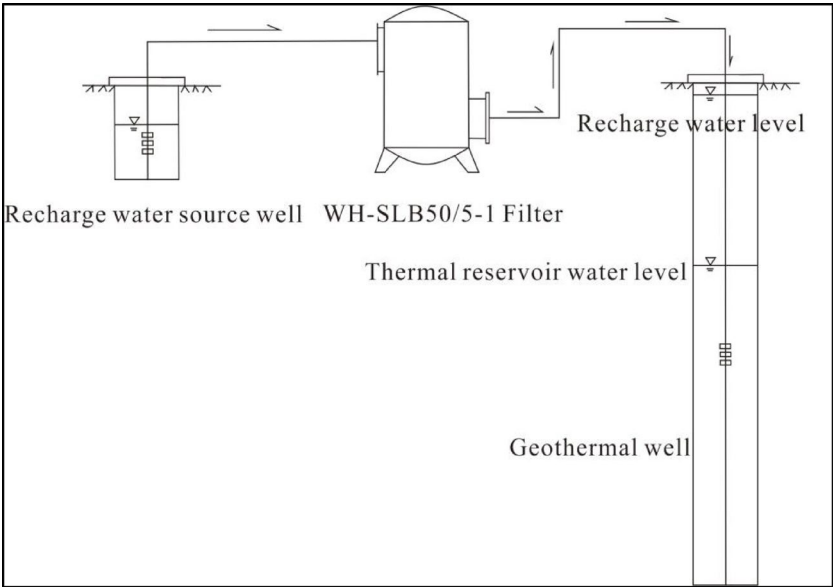

Fig. 3. Process flow diagram of reinjection.

thermal reservoir temperature is 60 °C.The chemical composition of geothermal water and recharge water is shown in Table 2.

The recharge source well is Na-HCO₃•SO₄•Cl type, and the Total Dissolved Solids(TDS) is 1.09 g/L. The geothermal water in the lower section of Minghua Town is Cl-Na type, and the TDS is 3.23 g/L. The two kinds of water quality are quite different, which may cause significant changes in the hydrochemical field of the thermal reservoir after recharge, and the recharge process is shown in Fig. 3.Four groups of recharge tests were carried out, and the duration curve is shown in Fig. 4.The water storage coefficient of thermal reservoir is S = 6.87 × 10⁻⁴ [3]. According to the recharge experiment, the average values of water injection permeability coefficient and water conductivity coefficient are obtained: K = 0.0783 m/d, T = 9.284 m²/d.

Model establishment and solution
Model establishment
Water flow movement

The thermal reservoir simulation object is the lower member of the Neogene Minghuazhen Formation, with a depth of 1061.65-1345.53 m, 7 water storage layers, and a total thickness of 118.52 m. It is a pressure-bearing thermal reservoir, and The thermal reservoir is set to be homogeneous and isotropic. The measured permeability is between 19.35×10^{-3} and $21.49 \times 10^{-3} \mu m^2$, and the permeability was set to $20 \times 10^{-3} \mu m$.

The gravity reinjection method is used to inject the hot reservoir. The reinjection head is 87.62 m according to the reinjection test, and the reinjection duration is 120 days.Considering that the flow velocity of recharge is much larger than the flow velocity of hot water in the geothermal reservoir, it is generalized as the static geothermal water in the reservoir. At the same time, the leaking recharge of adjacent strata is not considered. Under this premise, the recharge process can be generalized as a one-dimensional flow process with geothermal wells as the center and extending outward.

The water flow in the recharge period is calculated by the constant water level well flow formula (1). The water level in the process of head decline after the recharge stops is calculated by formula (2), and then substituted into formula (1) to calculate the flow after the recharge stops. The calculation period of the whole process is 1 year.

The well flow during recharge was calculated by using formulas (1) and (2).

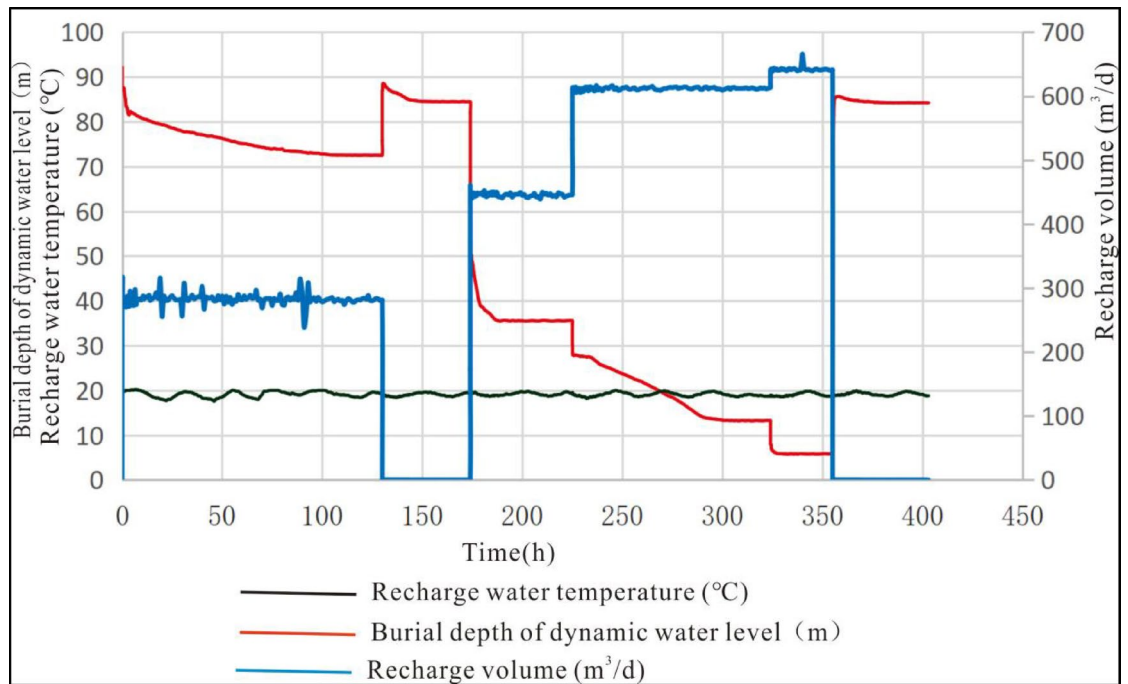$$Q_t = 2\pi \, KMswG\left(\frac{Tt}{Sr^2}\right) \tag{1}$$

4

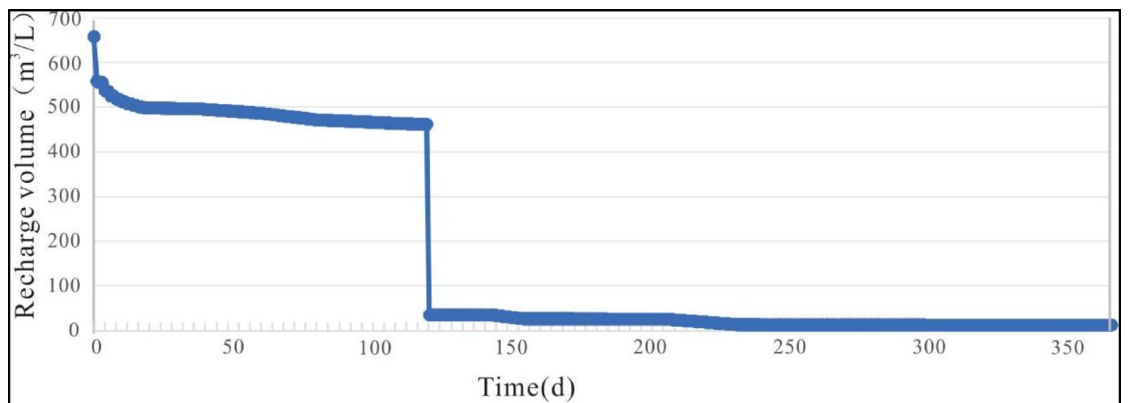**Fig. 4**. Duration curve of reinjection experiment.

Fig. 5. Recharge flow curve with time.

$$St' = \frac{Q'}{4\pi \, KM}\left[W\left(\frac{Sr^2}{4KMt}\right) - W\left(\frac{Sr^2}{4KMt\prime}\right)\right] \tag{2}$$

In the formula: Q_t is the recharge flow varying with time, K is the permeability coefficient obtained from the recharge test, M is the thickness of the thermal reservoir, S_W is the increase value of the recharge water level, G($\frac{Tt}{Sr^2}$) is the flow function of the constant head variable flow, t is the hydraulic conductivity coefficient, t is the time, S is the water storage coefficient, r is the well radius, $S_t\prime$ is the rising value of the remaining water level in the geothermal well after the recharge is stopped, $Q\prime$ is the flow at the moment before the recharge is stopped, and w($\frac{Sr^2}{4KMt}$) is the well function.

According to the above two formulas, the change of recharge flow is calculated as shown in Fig. 5. the recharge time is 120 days. During the fixed water level reinjection period, due to the rise of the water level around the geothermal well, the actual head difference gradually decreases, and the reinjection flow decreases accordingly. After 120 days of stopping reinjection, the flow path drops precipitously, but it is still not zero, and it remains basically stable after 180 days.

Solute transport and water mixing

After the shallow Quaternary groundwater recharges the thermal reservoir, the solute moves around the recharge well under the influence of water head difference and dispersion, and the velocity of convection is set according to the flow rate. Dispersion is a mass transfer process with scale effect. The dispersion is taken as 1 m this time[47]. According to the results of rock, water chemistry test and water-rock reaction experiment, calcite, dolomite, muscovite, chlorite, albite, kaolinite, illite, quartz and potassium feldspar are taken as the main reaction minerals. The dissolution and precipitation reaction formula is shown in Table 3.

The reaction amount is calculated according to the proportion of the reaction minerals in the rock samples of the thermal reservoir, and the reaction amount was calculated by formula 3.

$$M_r = \rho_r (V_w \div \in_p (1 - \in_p))$$ (3)

In the formula: M_r is the mass of rock (g), ρ_r is the density of rock (g/m³), V_W is the volume of reactive water (m³), and $\in_p$ is the porosity of rock (%).

According to the characteristics of water flow in the underground environment, the degree of contact between minerals and water often leads to the fact that minerals are not dissolved and precipitated in a saturated state. In this paper, the dissolution kinetic rate formula is used to characterize the dissolution and precipitation of minerals. The dissolution and precipitation of minerals were calculated by formula (4).

$$K^f = A^f exp\left(\frac{-E^f}{TR_g}\right)\left(\frac{T}{T_{ref}}\right)^{n^f}, T_{ref} = 1K$$ (4)

In the formula: K^f is the reaction rate constant; A^f is the frequency factor; E^f is the activation energy; R_g is the molar gas constant; T is the thermodynamic temperature.

Model and solution

According to the model described in Sect. 2.1, a one-dimensional convection dispersion equation is established to simulate the solute behavior of reinjection water in the thermal reservoir. The solute transport was calculated by formula (5)

$$\frac{\partial^2 C}{\partial t^2}D_L = \frac{\partial C}{\partial t} + v\frac{\partial c}{\partial x} + \frac{\partial q}{\partial t}$$ (5)

In the formula: $\frac{\partial^2 C}{\partial t^2}D_L$ is the concentration change caused by dispersion (mol m⁻³ s⁻¹), $\frac{\partial q}{\partial t}$ is the concentration change caused by water rock reaction (mol m⁻³ s⁻¹), $v\frac{\partial c}{\partial x}$ is the concentration change caused by flow (mol m⁻³ s⁻¹), and $\frac{\partial C}{\partial t}$ is the concentration change with time (mol m⁻³ s⁻¹).

The Transport module in PREEQC software is used to construct a radial one-dimensional solute transport reaction model with geothermal wells as the starting point. The dissolution kinetic rate formula (4) in the RATES _ Kinetic module is used to simulate the dissolution and precipitation of minerals, so as to calculate the concentration change caused by the reaction term in formula (5). At the same time, the temperature conditions of water-rock reaction with different mixing ratios of different water sources are set by Reaction _ Temperature module.

To verify the accuracy of the model, water quality samples were taken from the recharge well after the recharge was stopped. The test results are shown in Table 4.

The comparative analysis of cationic test results at 120d, 180d, and 360d with simulation outputs is presented in Fig. 6. As shown in the figure, the post-cessation monitoring data of recharge demonstrate close agreement with simulated values, indicating that the simulation results exhibit reasonable reliability in this study..

Analog setting

The volume of water rock reaction water is calculated by the formula (1) and (2). The front of the recharge water is continuously moving out of the well under the action of the hydraulic slope, and the original geothermal water in the thermal reservoir is gradually replaced by the recharge water. The front of the recharge water is

Reaction	Log_k	ΔH(kcal)
$CaCO_3 = CO_3^{-2} + Ca^{+2}$	8.48	2.297
$CaMg(CO_3)_2 = Ca^{+2} + Mg + 2 + 2\,CO_3^{-2}$	17.09	9.436
$KAl_3Si_3O_{10}(OH)_2 + 10\,H^+ = K^+ + 3Al^{+3} + 3H_4SiO_4$	12.99	59.34
$Mg_5Al_2Si3O_{10}(OH)_8 + 16\,H^+ = 5Mg^{+2} + 2Al^{+3} + 3H_4SiO_4 + 6H_2O$	68.38	151.494
$NaAlSi_3O_8 + 8\,H_2O = Na + + Al(OH)_4^- + 3\,H_4SiO_4$	18.002	25.896
$Al_2Si_2O_5(OH)_4 + 6\,H^+ = H_2O + 2\,H_4SiO_4 + 2\,Al^{+3}$	7.435	35.300
$K_{0.6}Mg_{0.25}Al_{2.3}Si_{3.5}O_{10}(OH)_2 + 11.2H_2O = 0.6\,K^+ + 0.25Mg^{+2} + 2.3Al(OH)_4^- + 3.5H_4SiO_4 + 1.2\,H^+$	40.267	54.684
$SiO_2 + 2\,H_2O = H_4SiO_4$	3.98	5.990
$KAlSi_3O_8 + 8\,H_2O = K^+ + Al(OH)_4^- + 3\,H_4SiO4$	20.573	30.820

Table 3. Mineral reaction parameters (20 ℃).

Sample time	K$^+$	Ca^{2+}	Na$^+$	Mg^{2+}	Cl$^-$	SO$_4$$^{2-}$	HCO$_3$$^-$
120d	0.110	3.08	25.3	0.60	2.55	1.30	4.74
150d	0.11	3.08	25.3	0.6	2.55	1.3	4.74
180d	0.092	2.30	25.5	1.40	2.83	1.52	4.70
240d	0.091	2.280	25.633	1.500	3.353	1.580	4.647
360d	0.088	2.24	25.9	1.70	4.40	1.70	4.54

Table 4. Sampling test results of recharge wells.
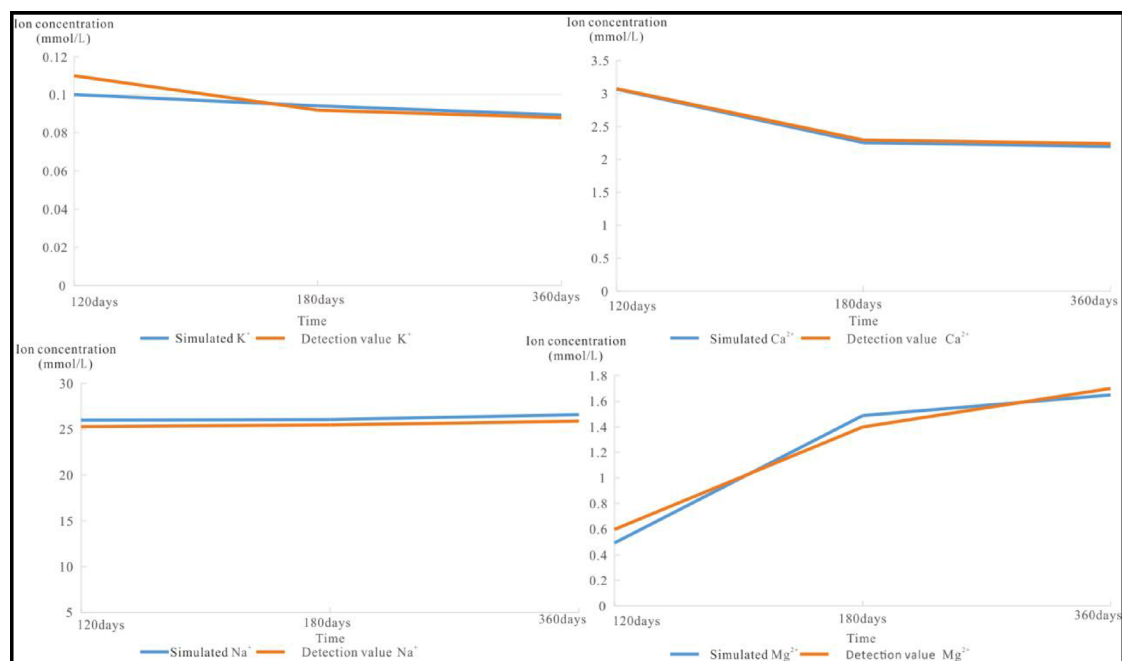
Fig. 6. Model validation results.

generalized as a cylinder with the geothermal well as the axis and the thickness of the thermal reservoir as the height. Because the radius of the geothermal well is quite different from the range of water quality migration, the radius of the geothermal well is ignored. The formula 5 ~ 7 is used to simplify the three-dimensional space into one-dimensional calculation of the position of the water flow front.

$$W_i = Q_i \times \Delta t_i \tag{5}$$

$$W_i = \pi M \times \in_p \times (R_i^2 \times R_{i-1}^2) \tag{6}$$

$$\Delta L_i = R_{i-1} + R_i \tag{7}$$

In the formula: W_i is the volume of reinjection liquid in time Δt_i (m^3), M is the thickness of thermal reservoir (m), $\in_p$ is the effective porosity of rock (%), and R_i is the radius of reinjection front at time t_i. ΔL_i is the length of migration path in time Δt_i. The schematic diagram is Fig. 7.

According to the water flow migration time in the Transport module, Table 5 is used to divide the time and space, and the total length of the effluent chemical path is calculated to be 55.75 m.

Results and discussion
Hydrochemical evolution and Spatial zonation in geothermal reservoirs
The simulation results of water chemical changes in the radial direction at different times are shown in Fig. 8. From the figure, it can be seen that the influence range of recharge water increases with time. At the end of the 120-day recharge, a total of 59,141 m^3 of recharge water is injected into the thermal reservoir. If all the recharge wells are filled around the recharge well, the radius of the filled aquifer is only 12.61 m, but the obvious variation range of the hydrochemical field of the thermal reservoir can reach 47.75 m. The content of Na$^+$, K$^+$ and Mg^{2+} increased gradually with the increase of radial distance until it was consistent with the content of geothermal water in thermal reservoir, However, Ca^{2+} showed a different trend of decreasing first and then increasing. The gradual increase of Na$^+$, Mg^{2+} and K$^+$ content is mainly due to the micro-dissolution of potassium feldspar, albite, illite and chlorite. The trend of Ca^{2+} is mainly caused by the precipitation of calcite around the recharge
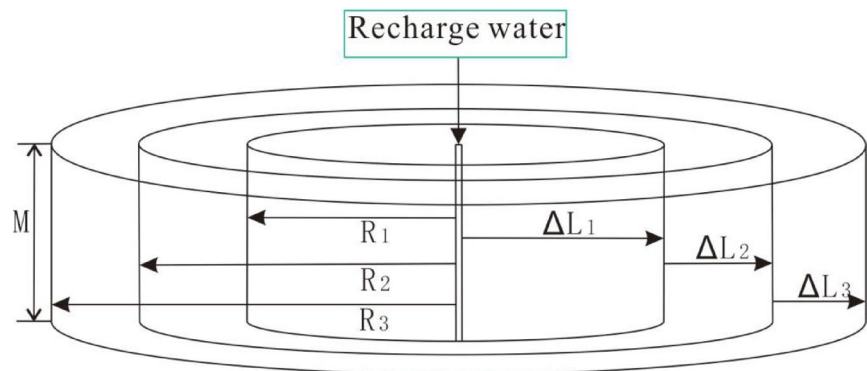
Fig. 7. Schematic diagram of reinjection water migration.

Total time(d)	Time(d)	Steps
1	0.5	1–2
	0.12	3–4
	0.28	5–6
2	0.43	7–8
3	0.50	9–10
4	0.72	11–12
5–6	0.90	13–14
7–12	1.00	15–20
13–21	1.50	21–26
22–33	2	27–32
34–53	2.5	33–40
54–77	3.0	41–48
78–91	3.5	49–52
92–115	4.0	53–58
116–120	5.0	59
121–360	120	60–62

Table 5. Time step division.

well. The maximum amount of precipitation is 7.25 m away from the center of the recharge well. After that, the precipitation reaction gradually weakens and returns to the normal value of the thermal reservoir at 17.5 m. This change is controlled by temperature, pH and recharge water pressure.

It can also be seen from Fig. 8 that there are areas with the same quality of reinjection water near geothermal wells in the figures of 10 days, 30 days, 60 days and 120 days, which increase with the extension of reinjection time, and this area is dominated by convective displacement. Then outward is the area dominated by dispersion, and the hydrochemical characteristics gradually transition to geothermal water until they are the same as geothermal water.After 120 days, the ion content in the water around the recharge well tends to increase (180 days and 360 days). This is due to the fact that as the recharge stops, the flow rate in the original convection zone of the thermal reservoir becomes smaller until it is stationary. The recharge in this area is mainly from flow to water-rock reaction, and the water-rock reaction leads to the change of ion content in the water around the recharge well.

According to the previous analysis, recharge time, recharge runoff velocity, recharge temperature, recharge water quality, reservoir composition, thermal reservoir type, geothermal water composition and so on all play a decisive role in the hydrochemical evolution of recharge.In the process of reinjection, the hydrochemistry around the reinjection well is mainly affected by the reinjection flow rate, and various water rock reactions are limited, showing consistency with the water quality of the reinjection water source. Afterwards, it is controlled by the combined action of convection mass, but mainly for dispersion. Different proportions of reinjection water and geothermal water are formed around the reinjection well until it reaches the boundary of reinjection influence and becomes the geothermal water quality of the thermal reservoir, as shown in Fig. 9. Therefore, reinjection can be divided into runoff influence zone, dispersion dominant zone, and unaffected in-situ geothermal water zone. Under the conditions of re irrigation water temperature, water quality, re irrigation time, and determination of the thermal reservoir, the hydrochemical type of the thermal reservoir is mainly controlled by runoff and dispersion during the re irrigation process. After the re irrigation is completed, it is controlled by water rock reaction and dispersion. Figure 10 is an evolution diagram of the hydrochemical type of 10 days, 30 days, 60
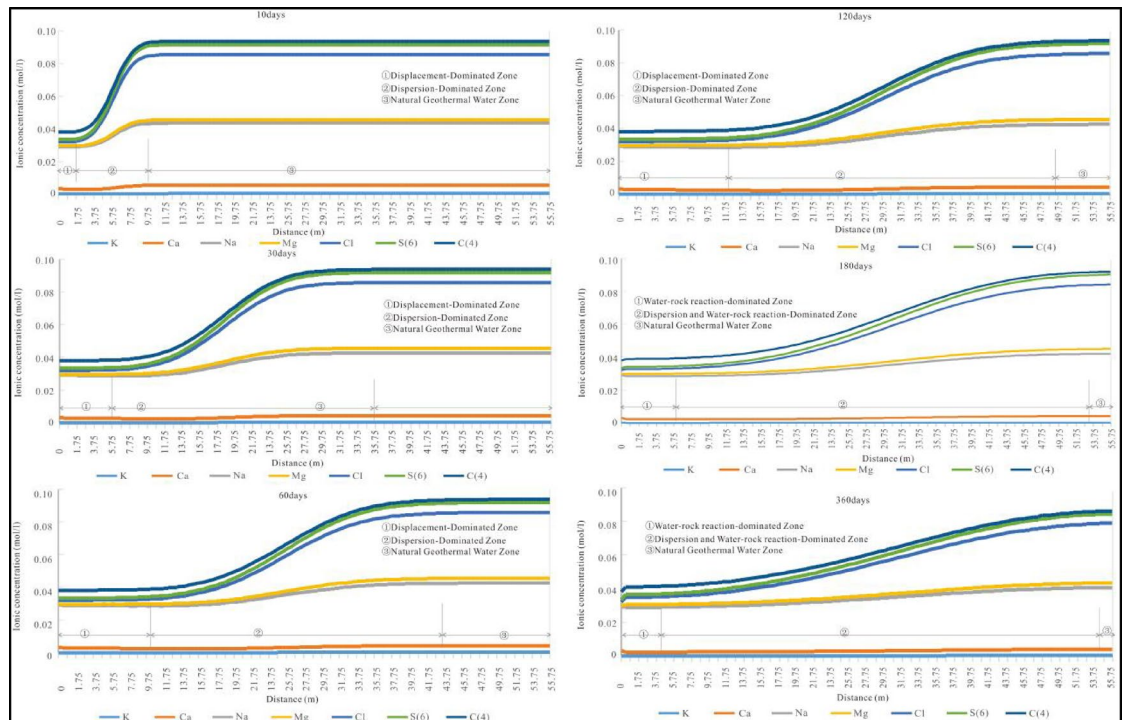
Fig. 8. Profile of hydrochemical evolution in 10, 30, 60, 120, 180 and 360 days.
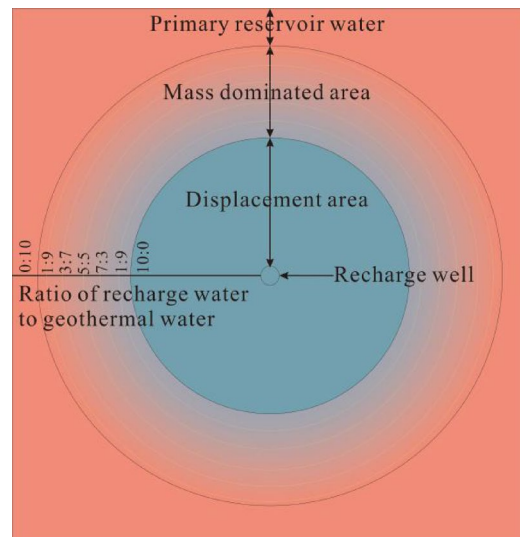

Fig. 9. Schematic diagram of impact zone division.

days, 120 days, 180 days and 360 days with a step of 0.5 m.On the 10th day, with the reinjection well as the center, the hydrochemical types are Na-HCO$_3$•SO$_4$•Cl、Na-HCO$_3$•Cl•SO$_4$、Na-Cl•HCO$_3$•SO$_4$ and Na-Cl in turn; From the 30th day to the 180th day, taking the reinjection well as the center, the hydrochemical types are Na-HCO$_3$•SO$_4$•Cl、Na-HCO$_3$•Cl•SO$_4$、Na-Cl•HCO$_3$•SO$_4$、Na-Cl•SO$_4$ and Na-Cl in turn; The 360 days were Na-Cl•HCO$_3$•SO$_4$、Na-Cl•SO$_4$•HCO$_3$、Na-Cl•SO$_4$ and Na-Cl.From the change of hydrochemical type before 180 days of recharge, it can be seen that the attenuation rate of HCO$_3$ is large, mainly because the Ca reaction in HCO$_3$ rock generates calcite, resulting in the supersaturated precipitation of calcite.At 360 days, the hydrochemical types of Na-HCO$_3$•SO$_4$•Cl and Na-HCO$_3$•Cl•SO$_4$ disappeared, the hydrochemical type dominated by Cl ions around the recharge well shows that the recharged groundwater gradually evolves into geothermal water quality under the influence of water-rock reaction.

Before the reinjection is stopped, the water of Na-HCO$_3$•SO$_4$•Cl type continues to expand around the reinjection well, and except for the primary water, the other hydrochemical types are less than this range.This
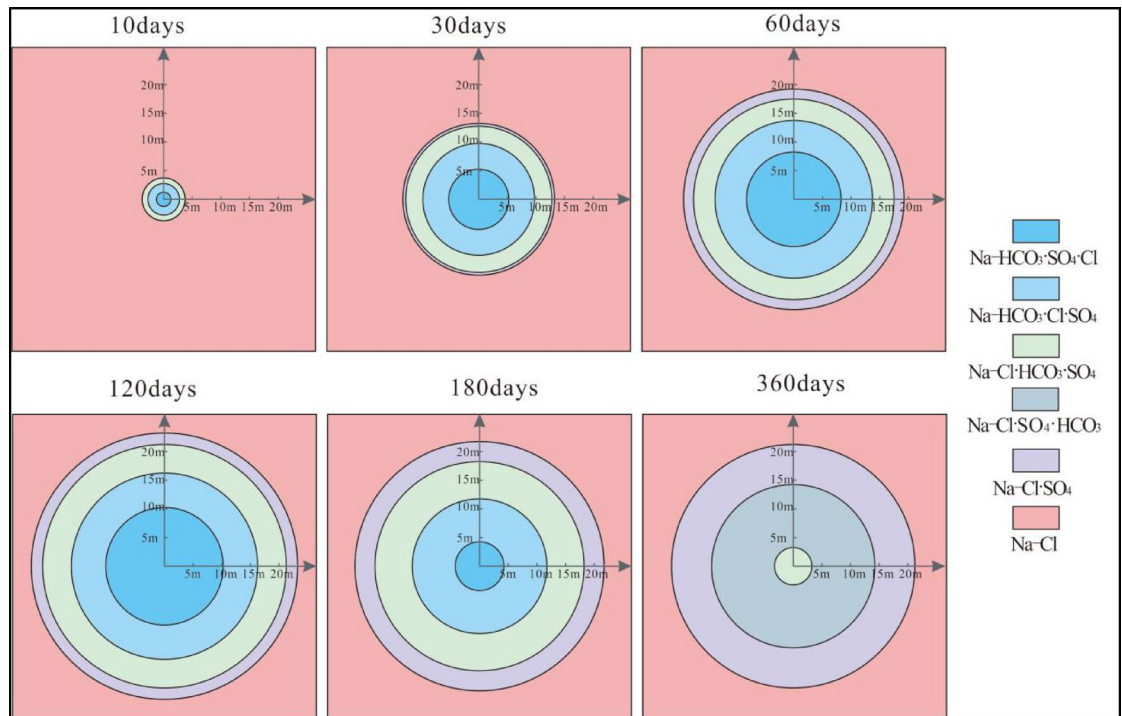
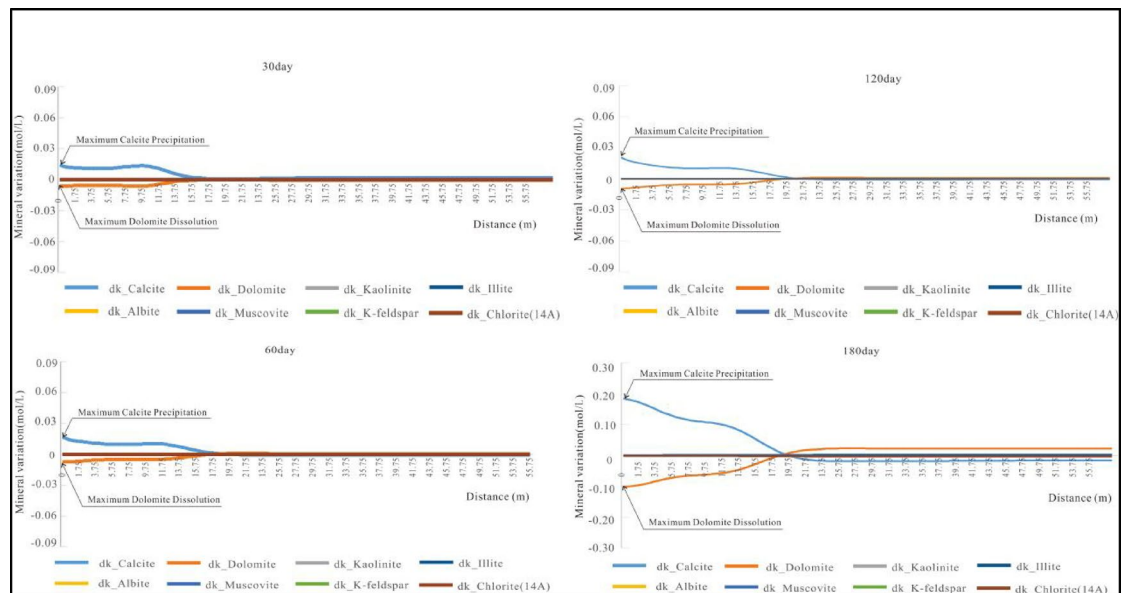**Fig. 10**. Evolution diagram of hydrochemical types.

Fig. 11. The mass change of minerals in thermal reservoirs for 30, 60, 120 and 180 days.

phenomenon shows that before stopping irrigation, the hydrochemical field around the recharge well is mainly affected by runoff, and the dispersion effect increases with the extension of recharge time.fter the reinjection stops, the water-rock reaction is the main reason for the change of the water chemistry type, which is manifested by the gradual narrowing and disappearance of the range of the chemical type of the reinjection.

Mineral reaction volume in reservoir

Figure 11 shows the amount of mineral reaction in the radial direction starting from the recharge well at different times. It can be seen from the figure that calcite precipitation mainly occurs after the start of recharge, while dolomite dissolves, and other minerals change very little. This result is consistent with the change of water chemical composition analyzed in Chap. 4.1.The obvious change range of minerals gradually expanded with the

progress of recharge reaction, 15.75 m at 30 days, 17.75 m at 60 days, and 19.75 m at 120 days.In the process of recharge, the change of minerals is small, that is, in the process of recharge, the surrounding area of recharge well is dominated by runoff.As the reinjection stops, the reaction around the reinjection well increases with the rise of temperature, and the dissolution of dolomite and the precipitation of calcite increase until a new water-rock balance is reached.Further calculation of the total amount of mineral changes in the thermal reservoir at 30 days is 7.43 g/ L, the total amount of mineral changes in the thermal reservoir at 60 days is 5.98 g/L, the total amount of mineral changes in the thermal reservoir at 120 days is 5.92 g/L, and the total amount of mineral changes in the thermal reservoir at 180 days is 56.67 g/L. It can be concluded that the total amount of minerals in the reservoir gradually decreases during the recharge process, but after the recharge stops, the amount of mineral precipitation increases significantly. It is speculated that the temperature has a control effect on the water-rock reaction. During the recharge, the temperature of the thermal reservoir gradually decreases, resulting in a decrease in the water-rock reaction and a gradual decrease in the precipitated minerals. When the reinjection stops, the reinjection area is in a static state soon, the temperature of the thermal reservoir rises slowly under the action of heat conduction, and the precipitation of calcite is enhanced. Another phenomenon should also be noted that the precipitation of this mineral dissolves most strongly near the recharge hole, and gradually weakens as it moves away from the recharge hole in the radial direction.

Taking the simulation results of the precipitation and dissolution of calcite within 11.25 m around the reinjection well on the 10th day of reinjection as an example, the t-test calculator was used to calculate $t = 25.1736$, $df = 44$, The standard error of the difference is 0.012, and the P value is less than 0.0001. The significant difference between the two indicates that there is a large difference in the precipitation amount of calcite and the dissolution amount of dolomite. The precipitation rate of calcite precipitation is much higher than that of dolomite dissolution, and this difference causes changes in the reservoir structure.

After the increase of mineral content, the new increase of minerals will occupy the original pore space, resulting in the decrease of porosity of thermal reservoir, which will affect the recharge performance of thermal reservoir. The volume change of each mineral can be calculated by the formation or dissolution of different minerals, and then the change of porosity can be calculated. The result is that the porosity decreases by 0.31% at 120 days, that is, the porosity decreases from 18.53% to 18.22%. At 180 days, the porosity decreases by 3.35%, that is, the porosity decreases from 18.53% to 15.18%(Table 6).

It can be seen that the recharge capacity of the thermal reservoir continues to decay when the reservoir continues to recharge, but the attenuation rate is slow; after the reinjection is stopped, the reinjection capacity of the reservoir is greatly attenuated. This is because there is recharge water around the recharge well, and the water-rock balance between recharge water and thermal reservoir rock is poor. During reinjection, this area is dominated by runoff, and after stopping reinjection, it becomes the area dominated by water-rock reaction with the increase of temperature.

In the actual recharge, there is heterogeneity in the thermal reservoir. This dissolution and precipitation also have heterogeneity, which may cause the structural change of the reservoir, and then cause the structural damage of the sandstone thermal reservoir, resulting in the ' collapse well ' accident.

From the perspective of long-term recharge, the quality of recharge water will have a significant impact on the porosity of the thermal reservoir, which in turn affects the permeability of the thermal reservoir. During the recharge process, attention must be paid to the impact of recharge water quality on the physical properties of the thermal reservoir.

Temperature change in thermal reservoir

Figure 12 shows that the temperature around the reinjection well gradually decreases with the increase of the reinjection time of the low temperature water.The influence range of temperature is 7.75 m at 10 days, 24.75 m at 30 days, 33.75 m at 60 days, 39.25 m at 120 days, 48.25 m at 180 days, and 57.25 m at 180 days.It can be shown that the expansion rate of temperature effect decreases with time.After 120 days of recharge, the area around the recharge well changed from gradually decreasing to gradually increasing, but the increase was far less than the

120days				180days			
Mineral	Variation (g/L)	Density(g/cm³)	Volume change(%)	Mineral	Variation (g/L)	Density(g/cm³)	Volume change(%)
Calcite	33.93	2.60	13.05	Calcite	264.75	2.60	101.83
Dolomite	-23.81	2.70	-8.82	Dolomite	-109.35	2.70	-40.50
Kaolinite	0.00	2.63	0.00	Kaolinite	0.05	2.63	0.02
Albite	0.00	2.62	0.00	Albite	-0.08	2.62	-0.03
Muscovite	4.38	2.76	1.59	Muscovite	96.66	2.76	35.02
K-feldspar	0.00	2.57	0.00	K-feldspar	-0.01	2.57	0.00
Illite	-0.01	2.75	0.00	Illite	-0.26	2.75	-0.09
Chlorite(14 A)	-8.22	3.13	-2.63	Chlorite(14 A)	-187.57	3.13	-59.93
Quartz	-0.34	2.65	-0.13	Quartz	-7.52	2.65	-2.84
Amount to			0.31	Amount to			33.47

Table 6. Volume change of each mineral in 120 and 180 days. Note: "+" represents mineral precipitation or volume increase, "-" represents mineral dissolution or volume decrease.
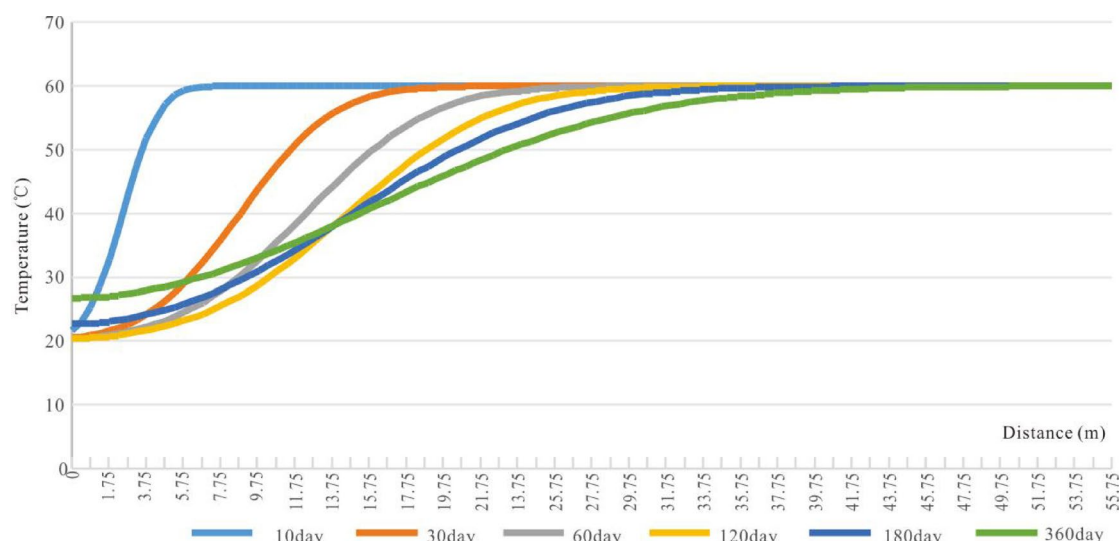
Fig. 12. Evolution profile of temperature field in 10, 30, 60, 120, 180 and 360 days.

decrease.It is worth noting that after the end of the reinjection, in the radial direction of the reinjection well, the thermal reservoir is not all manifested as a temperature rise, but the formation of two zones with a boundary of 14.75 m. The temperature gradually increases within 14.75 m, and the temperature outside the heat conduction will still gradually decrease. The primary limitation of this simulation lies in its neglect of thermal conduction effects external to the thermal reservoir. This omission may result in a marginally accelerated temperature decline rate compared to field observations. However, given the overwhelming influence of cold water injection on thermal dynamics, such discrepancies remain within acceptable tolerances for practical reservoir management purposes.

Conclusion

In this paper, the hydrochemical simulation model of shallow groundwater recharge to deep thermal reservoir is constructed, and the hydrochemical changes of thermal reservoir caused by recharge are analyzed by taking Yancheng uplift as the application site. The main results are as follows :

(1)Through the previous water sample, core sample test and recharge test, the main physical parameters of the thermal reservoir were determined, and the heterogeneous water recharge geological model of the thermal reservoir was constructed.

(2) The reinjection of the thermal reservoir is generalized as a one-dimensional radial water quality movement process along the reinjection well. The migration process is dominated by flow at first, and gradually evolved to mass at the periphery. The water rock reaction is dominated by the dissolution of dolomite and the precipitation of calcite, and the reaction amount of other minerals is very small. During the reinjection process, the reaction intensity near the reinjection well is the largest.

(3) With the progress of recharge, the reservoir will be damaged, which shows that the total amount of minerals in the reservoir shows an increasing trend. The main influence range is within 19.75 m, and the reservoir permeability will decrease, which is more obvious after stopping recharge. The porosity is reduced to 0.31% at 120 days and 3.35% at 180 days, accompanied by a decrease in reservoir temperature.

(4) The influence area of thermal reservoir recharge is divided into complete displacement area, mass dominant area and in-situ hot water area along the radial direction. The hydrochemical types of groundwater in different time and different range around the recharge well are discussed.

In summary, this paper uses the dissolution kinetic rate formula to construct the hydrochemical evolution model of porous thermal reservoirs under recharge conditions, and takes the thermal reservoir of Minghuazhen Formation in Yancheng uplift as an example to solve. Although the temperature rise caused by the heat conduction of adjacent strata is neglected, it can still provide important theoretical support for the study of water environment changes in thermal reservoirs caused by heterogeneous water recharge.

Data availability

The data supporting the results of this study are presented in this study.

References
1. Wnag, G., et al. The status and development trend of geothermal resources in China[J]. *Earth Sci. Front.* **27** (1), 001–009 (2020).
2. Xing, W., The Priority Sequence of New Energy Development in China until 2030[D],*ChinaUniversity of Geosciences* (2015).

3. Zhao M.,The Genesis Mechanism and Multi-field Evolution Driven by Heat Extraction of the Minghuazhen Formation Geothermal Reservior in Yancheng Uplift[D]*China University of Mining and Technology*. (2022).
4. Li, N., et al. Development trend and hotspot analysis of geothermal energy based on bibliometrics [J]. *J. Environ. Eng.* **32**, (10) 2746–2753 (2024).
5. Wang, G., Lin W., Special Editor's Letter to Readers: New Theories, Technologies, and Methods for Geothermal Exploration and Extraction towards Carbon Neutrality[J]. *Frontiers in Geosciences* **31**, (06) 5–8(2024).
6. Li, S., et al. Numerical simulation and analysis of the chemical evolution of Baiyangdian surface water injection in deep karst geothermal reservoirs in xiong'an new Area[J]. *China Environ. Sci.* **21** (2), 1–10 (2014).
7. Du, Y., et al. Characteristics of Sand Geothermal Reservoir and Fluid Chemical Characteristics of Dongying Formation in Northwestern Shandong Province[J]. *Caol Geology of China* **36**(04), 45–49 (2024).
8. Zhao M., et al. Geochemical Signature and Genesis of Geothermal Water in Minghuazhen Formation, Luohe, Henan Province[J]. *Geoscience* **36**(2), 507–514 (2022).
9. Liu, W.,et al. Development Potential and Environmental Benefit Analysis of Geothermal Medium–Deep Buried Pipe Heating System in Capital Cities in Northwest China[J]. *NW Geol.* **56**(03), 186–195 (2023).
10. Wang, Y., et al. The hydrochemical characteristics of geothermal water and its formation in the south Langfang, Hebei Province[J]. *Geol. Bull. China* **41** (9), 1698–1706 (2022).
11. Wang, G., et al. Discussion on the potentialassessment method of geothermal resources under balanced produetion and reiniection: A case study for the carbonate Reseryoi in xiong'an new Area[J]. *Acta Geol. Sinica.* **98** (6), 1928 (2024).
12. Liu, Y. Wang, G., Zhu Xi, et al.Occurrence of geothermal resources and prospects for exploration and development in China[J]. *Energy Explor. Exploit.* **39** (19), 014459871989582 (2019).
13. Zhang, M., et al. Theory and method for urban–Rural Integration, evaluation and cooperative detection of ground and underground space: example from the urban geological survey of Guanzhong Plain[J]. *Northwest Geology*,**56**, (03) 153–168 (2023) .
14. Lund, W. J., Freeston, H. D. & Geothermics World-wide direct uses of geothermal energy 2000[J].*Geothermics.* **30**, (1) 29–68. (2001).
15. Benoit, D., Johnson, S. & Kumataka, M. Development of an injection augmentation program at the Dixie Valley, Nevada geothermal field[C]. Proceedings of the World Geothermal Congress 2000. Kyushu-Tohoku, Japan. 819–824. (2000).
16. Sifford, A. Geothermal electric power production in the United States:A survey and update for 1995–1999[C]. Proceedings of the World Geothermal Congress 2000. Kyushu-Tohoku, Japan.441–453. (2000).
17. Lund, J. and T Boyd.Geothermal direct-use in the United States update:1995–1999[C]. Proceedings of the World Geothermal Congress 2000. Kyushu-Tohoku, Japan. 297–305. (2000).
18. Thain, I. and M Dunstall.1995–2000 update report on the existing and planned use of geothermal energy for electric- ity generation and direct use in New Zealand[C]. Proceedings of the World Geothermal Congress 2000. Kyushu-Tohoku, Japan.217–228. (2000).
19. Axelsson, G. et al. Thermal energy extraction by re-injection from the Laugaland geothermal system in N-Ice- land[C]. Proceedings of the World Geothermal Congress 2000. Kyushu-Tohoku, Japan.3027–3032. (2000).
20. Ragnarsson, A. Geothermal development in Iceland 1995–1999[C]. Proceedings of the World Geothermal Con- gress 2000. Kyushu-Tohoku, Japan.363–375. (2000).
21. Cappetti, G. G., Passaleva & Sabatelli, F. Italy country update report 1995–1999[C]. Proceedings of the World Geothermal Congress 2000. Kyushu-Tohoku, Japan.108–116. (2000).
22. Carella, R. & Sommaruga, C. Geothermal space and agri-business heating in Italy[C]. Proceedings of the World Geothermal Congress 2000. Kyushu-Tohoku, Japan.117–122. (2000).
23. Fuchino, H. Status of geothermal power generation in Japan[C]. Proceedings of the World Geothermal Congress 2000. Kyushu-Tohoku, Japan.193–198. (2000).
24. Goto, H. The decrease of capacity in re-injection wells in the Takigami field, Japan[C]. Proceedings of the World Geothermal Congress 2000. Kyushu-Tohoku, Japan. 3059–3063. (2000).
25. Hisatani, K. et al. The mixing of the cooling waste reinjected with the production flu- id at the Uenotai geothermal power station[C]. Proceedings of the World Geothermal Congress 2000. Kyushu-Tohoku, Japan. 3071–3075. (2000).
26. Kiyota, Y. et al. Evaluation on geothermal injection treatment by pH modification[C]. Proceedings of the World Geothermal Congress 2000. Kyushu-Tohoku, Japan. 3077–3082. (2000).
27. Cohut, I. & Bendea.Romania, C. Update report for 1995–1999[C]. Proceedings of the World Geothermal Congress 2000. Kyushu-Tohoku, Japan. 147–152. (2000).
28. Karunungan, V. and R Requejo.Update of geothermal development in the Philippines[C]. Proceedings of the World Geothermal Congress 2000. Kyushu-Tohoku, Japan. 247–252. (2000).
29. Teklemariam, M. et al. Geothermal development in Ethiopia[C]. Proceedings of the World Geothermal Congress 2000. Kyushu-Tohoku, Japan. 475–480. (2000).
30. Mahler, A. Geothermal plant with efficient absorption heat pumps driven by incineration CHP plant.Successful in- jection in sandstone aquifer.Country update Denmark[C]. Proceedings of the World Geothermal Congress 2000. Kyushu-Tohoku, Japan.307–312. (2000).
31. Mainieri, A. Costa Rica country update[C]. Proceedings of the World Geothermal Congress 2000. Kyushu-To- hoku, Japan. 313–318. (2000).
32. Mwangi, M. Country update report for Kenya 1995–1999[C]. Proceedings of the World Geothermal Congress 2000. Kyushu-Tohoku, Japan. 327–335. (2000).
33. Jelic, K., Cubric, S., Pavicic, H. & Bosnjak, R. Geothermal energy potential and utilization in the Republic of Croatia[C]. Proceedings of the World Geothermal Congress 2000. Kyushu-Tohoku, Japan. 237–246. (2000).
34. Quijano-Leon, J. & Gutierrez-Negrin, L. Geothermal production and development plans in Mexico[C]. Proceedings of the World Geothermal Congress 2000. Kyushu-Tohoku, Japan. 355–361. (2000).
35. Rodriquez, J. Geothermal development in El Salvador-A country update[C]. Proceedings of the World Geothermal Congress 2000. Kyushu-Tohoku, Japan.403–406. (2000).
36. Kononov, V., Polyak, B. & Kozlov, B. Geothermal development in Russia: country update report 1995–1999[C]. Proceedings of the World Geothermal Congress 2000. Kyushu-Tohoku, Japan. 261–266. (2000).
37. Laplace, P. et al. The French geothermal experience review and perspectives[C]. Proceedings of the World Geothermal Congress 2000. Kyushu-Tohoku, Japan. 283–295. (2000).
38. Seibt, P. & Markus Wolfgramm. Markus Wolfgramm."Practical experience in the reinjection of thermal waters into sandstone". Presented at the Workshop for Decision Makers on Direct Heating Use of Geothermal Resources in Asia.Ed.GTN-Geothermie Neubrandenburg GmbH Seestrasse 7 A 17033 Neubrandenburg GERMANY,202–219(2008).
39. Wei Song, X. et al. A review of recharge and clogging in sandstone aquifer[J],*Geothermics.* 87, 101857(2020).
40. Li, H. et al. Engineering Practice of Geothermal Recharge Technology For Leling Sanstone Thermal Storage[J]. *Therm. Sci.* **27**(3B), 2525–2536 (2023).
41. Mohammad Mirzavand, H. et al. Delineating the source and mechanism of groundwater salinization in crucial declining aquifer using multi-chemo-isotopes approaches[J]. *J. Hydrology*.**586**(3B), 124877 (2020).
42. Cobos, J. E. & Søgaard, E. G. Impact of reservoir heterogeneity on diluted geothermal Brine reinjection[J]. *Energies.* **15** (9), 3321 (2022).

43. Brehme, M. et al. Demonstration of a successful soft chemical stimulation in a geothermal sandstone reservoir in Mezőberény (Hungary). *Geothermics.***120**, 102980 (2024).
44. Li Shengtao, S. et al. Numerical simulation and analysis of the chemical evolution of Baiyangdian surface water injection in deep karst geothermal reservoirs in xiong'an new Area.[J]. *China Environ. Sci.* **21** (2), 33–42 (2024).
45. Xue, M. P., Zhang, Z. J. & Zhao, Y. Hydrochemical evolution of mine water injection in Hojirt mining Area[J]. *Coal Sci. Technol.* **51** (S1), 470–476 (2023).
46. Shao, M. et al. Spatiotemporal dynamics of ecosystem services and the driving factors in urban agglomerations: evidence from 12 National urban agglomerations in China[J]. *Front. Ecol. Evol. 2022 DOI* :https://doi.org/10.3389/fevo.2022.804969
47. Simulation and Prospect of Pore Type Geothermal Tail Water. *Reinjection in Sanqiao District of Xi'an—A Case Study of Geothermal Reinjection Wells* (of Huisen Company[D].Chang'an University, 2018).

Acknowledgements

Author contributions

ZMK analyzed the data and wrote the paper; DZF and JM revised the paper and guided the execution of the injection test; YH and QYJ do experiments and statistically analyze the experimental results; DXC and QSF participate in the drawing of graphics; BGX and TX participated in the numerical simulation of papers.

Declarations

Competing interests

The authors declare no competing interests.

Additional information

Correspondence and requests for materials should be addressed to J.M. or D.Z.

Reprints and permissions information is available at www.nature.com/reprints.

Publisher's note Springer Nature remains neutral with regard to jurisdictional claims in published maps and institutional affiliations.